Theoretical Study of the Human DNA Repair Protein HOGG1 Activity

Patric Schyman,† Jonas Danielsson,† Miroslav Pinak,‡ and Aatto Laaksonen*,†

Division of Physical Chemistry, Arrhenius Laboratory, Stockholm University, 106 91 Stockholm, Sweden, and Health Physics Department, Japan Atomic Energy Research Institute, Shirakata, Shirane 2-4, 319-1195 Tokai-mura, Ibaraki-ken, Japan

Received: September 22, 2004; In Final Form: December 14, 2004

We have examined the role of the catalytic lysine (Lys 249) in breaking the glycosidic bond of 8-oxoguanine in the enzyme human 8-oxoguanine DNA glycosylase. Until quite recently it has been assumed that this lysine acts as a nucleophile in an S_N2 type of reaction after being activated through a donation of a proton to a strictly conserved aspartate, also located in the active site. However, evidence from crystallographic, as well as biochemical studies, questions this assumption mainly because the lysine is not ideally positioned for such an attack. In addition, the catalytic activity is preserved even after that aspartate is mutated to a residue not accepting protons, but still keeping the interactions in the active site. In this study, we have investigated several different reaction mechanisms to discover plausible ways where the lysine could assist in breaking the glycosidic bond. We use hybrid density functional theory to characterize both associative and dissociative pathways. We find that the smallest energetical barrier involves an S_N1 type of mechanism where the lysine electrostatically stabilizes the dissociating base and then donates a proton with a very small barrier and then finally attacks the sugar ring to create the covalently bound protein−DNA intermediate complex. The S_N2 mechanism also has a lower barrier than the "spontaneous" bond breaking but considerably above that of the S_N1 reaction. However, in current conditions, the reactants placed in a conformation posed for an S_N2 reaction is substantially more stable than if posed for the S_N1 reaction, indicating that the active site has to bind stronger to the latter in order to achieve a full catalytic effect. An analysis of the polarization of the transition states shows that the polarization is largest for the S_N1 reaction, indicating that this path will gain most by being placed in a prepolarized active site. These findings give further support to the hypothesis that a dissociative mechanism may be the preferred mode of action for this type of enzymes.

Introduction

The ability of the human cell to repair chemically and physically damaged DNA is crucial to maintain the integrity of the information stored in the genes. To achieve this, a large repertoire of DNA repair proteins has evolved. One of these is the human 8-oxoguanine DNA glycosylase, abbreviated hOGG1, excising the oxidated form of guanine, 7,8-dihydro-8oxoguanine (8-oxoG).[1−4] The oxidation is a chemical modification caused by reactive oxygen species (ROS),[5] generated from ionizing radiation or UVA exposure through, e.g., sunlight,[6] but also organic free radicals,[3,7] caused for example by tar and tobacco smoke.[8] ROS damaged guanine can also be produced as a byproduct in normal cellular metabolism.[4]

The formation of 8-oxoG frequently leads to a permanent alteration of the DNA base sequence.[9] In the Watson−Crick mode, guanine pairs with cytosine, forming a G:C pair, but 8-oxoG can also form a Hoogsteen pair with adenine, 8-oxoG:A. The next round of 8-oxoG:A replication produces a thymine−adenine pair (T:A).[10] The G:C → T:A transversion mutation is one of the most common somatic mutations in human cancer.[11,12]

The hOGG1 specifically recognizes the 8-oxoG:C pair and binds the 8-oxoG into its active site pocket.[7,13] The mechanism is not clarified yet. There are several hypotheses how the hOGG1 protein recognizes the 8-oxoG. One suggestion is that the hOGG1 is sliding along the DNA in the search for 8-oxoG.[14] When the protein finds the oxidative damaged guanine, it will pull the damaged base out and into the active site. According to an alternative suggestion, the 8-oxoG lesioned base can spontaneously flip out[13,15] of the helix, and the hOGG1 will recognize it in this state. Molecular dynamics simulations of B-DNA, where a native guanine in the central part of the 15-mer was replaced by 8-oxoG, give some support for the latter suggestion.[16] Furthermore, the structures of the hOGG1−DNA complex, obtained from the X-ray experiments,[7,13,17,18] provide important information on how this DNA repair protein binds 8-oxoG into the active site. A detailed inspection of the active site (see Figure 1) shows

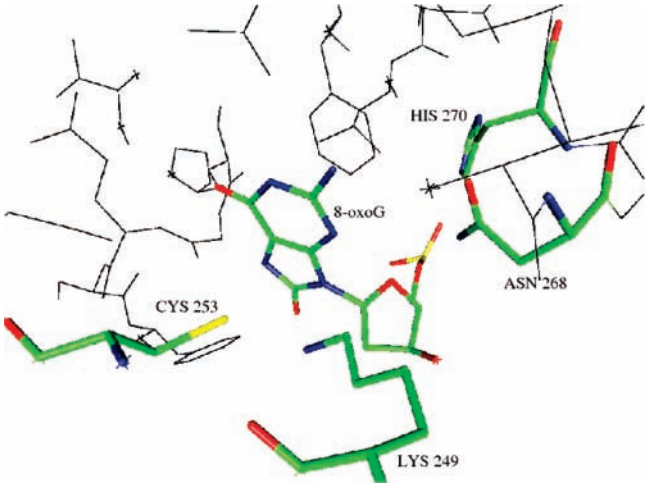

Figure 1. The active site for the 1N3C structure showing the residues that interacts with 8-oxoG.

* Corresponding author.
† Stockholm University.
‡ Japan Atomic Energy Research Institute.

10.1021/jp045686m CCC: $30.25 © 2005 American Chemical Society
Published on Web 02/05/2005

that a lysine (Lys249) has a favorable position for an attack and enables the enzyme catalysis of the glycosidic bond between 8-oxoG and the ribose ring. It has also been shown by mutation experiments that this residue is crucial for enzymatic activity.[17]

However, it is not clear yet how the hOGG1 catalyses the excision of the 8-oxoG. To use Lys 249 as a nucleophile, this residue has to be activated by deprotonation. It was assumed that aspartate (Asp268), conserved in the hOGG1 of the HhH-GPD superfamily would have this role. However, mutation experiments revealed that substantial catalytic activity remains even if Asp 268 is replaced by amino acids that cannot perform this kind of chemistry, such as aspargine (Asn) and glutamine (Gln).[17] The results of these findings have raised new questions on the catalytic mechanism and the role that Asp plays. From these mutation experiments, Asp instead seems to have an important structural role when capping the α-helix, and possibly provide some electrostatic stabilization of the transition state.[17]

Bifunctional DNA glycosylases are characterized by the presence of a catalytic lysine in the active site, where the lysine forms a Schiff base with the ribose ring after the glycosidic bond break.[20] In this paper, we have investigated two types of catalytic reaction mechanisms involving Lys 249, one of dissociative S_N1 type and the other with a associative S_N2 kind of mechanism. In this initial study of a model system of the protein, using quantum chemistry calculations on a small subsystem, we wish to obtain some insight on the reaction involving the catalytic lysine. To the best of our knowledge, no quantum chemistry methods have been previously applied on this system.

To compare the dissociative and the associative catalytic mechanisms with each other, we used three DNA−hOGG1 complex structures, labeled 1N3C, 1EBM, and 1FN7 in the Protein Data Bank entry code. The 1N3C structure suggest a dissociative S_N1 reaction, such mechanism have been found in similar enzymes, e.g., uracil−DNA glycosylase.[19] The residue Asp 268 in this structure is mutated to Asn 268 and is unable to deprotonate Lys 249. The second structure, 1EBM, we have replaced glutamine with lysine. The S_N2 reaction can be studied in the 1FN7 structure, since Asp 268 has a favorable position in the active site to deprotonate Lys 249 for a nucleophilic attack.

Models and Computational Details

The models used of the 8-oxoG in the hOGG1 active-site pocket, were obtained from high-resolution crystallographic structures with codes 1N3C, 1EBM, and 1FN7 in the Protein Data Bank (PDB). The abbreviations used for the structures and residues associated e.g. Lys 249 is the same as those in the PDB. In the 1N3C structure, a complex of hOGG1 and 8-oxoG as a substrate, the hOGG1 aspartate (Asp) has been mutated to aspargine (Asn) at the position 268.[17] For the 1EBM structure, with the 8-oxoG-hOGG1 complex, the lysine is mutated to glutamine (Glu) at position 249.[7] In this mutated form of hOGG1 we have replaced Glu with Lys and positioned under the sugar ring on the opposite side of the 8-oxoG, since in its crystallized form it shows no catalytic activity at the active site.[20] The 1FN7 structure uses a complex without 8-oxoG but instead using the wild-type hOGG1 and the tetrahydrofuranyl (THF) as substrate.[21] In our model we have implemented the 8-oxoG into the 1FN7 structure.

The 1N3C, 1EBM, and 1FN7 structures provide initial coordinates for the two suggested catalytic processes S_N1 and S_N2. The dissociative S_N1 mechanism seems to be most likely by a detailed inspection of the 1N3C and 1EBM structures. The Lys 249 in the 1N3C is not able to become deprotonated, since Asp 268 is mutated to Asn 268. The active site of the 1N3C structure in Figure 1, shows the residues that interact with 8-oxoG. In the 1FN7 structure the Lys 249 is suited for an S_N2 reaction, acting as an attacking nucleophile.

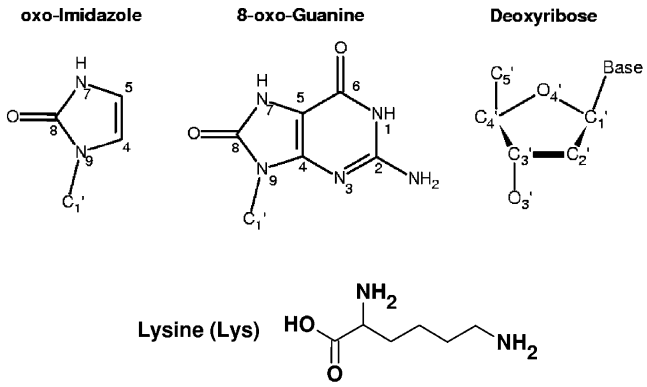

Figure 2. Molecular fragments used in our models with numbering.

At this first stage of investigating these mechanisms, the surrounding residues have not been taken into account, even though their presence may not be negligible. The 8-oxoG base in the real reaction has been simplified in our computational models to oxo-imidazole except in the section Extended System, where the effect of the omitted part of the guanine is analyzed. Since it should not have any major impact on the involved chemistry (and also to avoid confusion), we will still refer to oxo-imidazole as 8-oxoG. In Figure 2, 8-oxoGuanine, oxo-imidazole, and deoxyribose are presented with atomic labels used in this report.

All calculations were performed with Gaussian 98.[22] The energy surface was investigated with the B3LYP hybrid functional[23−25] using 6-31G(d) basis set. To find stationary points, we have used the synchronous transit-guided quasi-Newton (STQN) method with the QST3 option,[26] which requires the reactant, product, and initial transition state structures as an input. Furthermore, frequency calculations carried out at the stationary points and the successful location of a transition state (TS) was thereafter verified by the existence of an imaginary frequency. Intermediate structures, reactants, and products have been energy optimized. Single point calculations with the 6-31+G(d,p) basis set containing both polarization and diffuse functions, were preformed on all optimized structures to calculate energies and partial charges. The partial charges were obtained from natural bond orbital (NBO) analysis[27] carried out with Gaussian 98.[22] The distances between the atoms connected to the backbone were locked in the 1N3C model (model A). During the energy optimization of the reactant structure of model A, the dihedral angle (O4′−C1′−N9−C4) was fixed to prevent an unrealistic conformation of the structure which would not be possible in the active site. For the other models no coordinates were locked. The validity of these methods and the B3LYP functional for similar systems have been tested and shown to agree quite well with experiments.[28] The proton affinity (PA) of the different products was calculated at 298 K with the formula

$$P(A) = -\Delta E_{el} - \Delta ZPE + \frac{5}{2}RT$$

The B3LYP/6-31+G(d,p) was used to calculate E_{el} and ZPE.

Results and Discussions

The three different structures 1N3C, 1EBM, and 1FN7 and the different conclusion about the role of Lys 268 motivated us to investigate the energy surfaces of the two mechanistic proposals, S_N1 type and S_N2 type in hope to shed light on the pro-

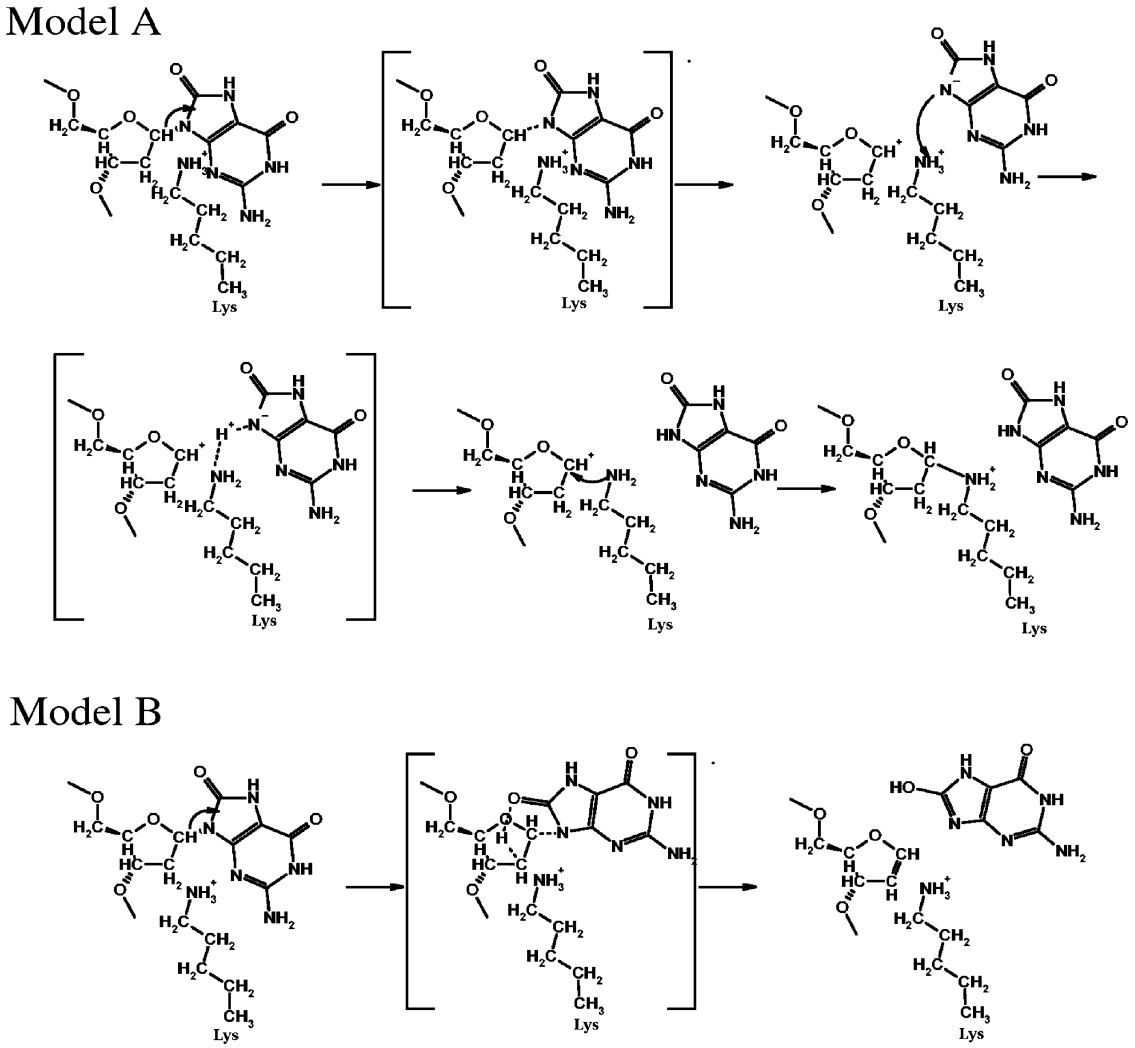

Figure 3. Two reaction pathways A and B that have been suggested from the X-ray structures. The reaction scheme also includes TS structures. Models A and B are S_N1 reactions with a passive lysine located beside respectively on the opposite side of the 8-oxoG. The reaction for model Basic is similar to model B's but without the lysine.

cess. The position of the Lys 249 side chain in our computational models was determined with help of these structures.

The models are hereafter labeled as A (1N3C), B (1EBM), and C (1FN7), with the corresponding original structure in the parentheses. The three main reaction paths with Lys 249 are shown in Figures 3 and 4. Pathways A and B are S_N1, and pathway C is an S_N2 reaction. These models are then compared with the Basic model without the lysine, to evaluate the catalytic influence it has in the different models. The reaction pathway for model Basic is similar to the reaction of model B but without the lysine (see Figure 3). First we will present the result from our calculations with the different reaction mechanisms and pathways. The energies for all reaction steps that will be discussed in the following text are summarized in Table 1, including ZPE correction and energies obtained from single-point calculation with the basis set 6-31+G(d,p).

In the section Extended Systems below, we have recalculated the TS energy for the different mechanisms, but then using the whole 8-oxoG instead of our simplified guanine model (imidazole), and these results are presented in Table 2. In the end, proton affinity and charge distribution during the reaction are in focus.

S_N1 Type Mechanism. The energetic of S_N1 reaction were obtained for three models, Basic, A, and B, to get insight in the glycosylase activity. The energy diagram obtained for pathway A and B are depicted in Figure 5, and in Figure 6, the transition state structures are presented with bond distances.

S_N1 Pathway Basic. In the first Basic model (the simplest reference case) of 8-oxoG binding to the sugar ring, the enzyme has not been introduced. The different reaction steps can be followed in Figure 3 (referring to model B but without the lysine). The dissociation energy barrier of 8-oxoG, without the lysine, gives a TS of 45.34 kcal/mol and a product of 25.39 kcal/mol, relative the initial energy. At the TS when the 8-oxoG excises, the distance between the sugar ring C1′ and the 8-oxoG's N9 is 2.50 Å. The O8 of 8-oxoG is protonated with a hydrogen from the C2′ of the sugar ring during the dissociation. In the initial structure of 8-oxoG, the C8 and N9 are connected with a single bond (1.40 Å) while the C8 and O8 has a double bond (1.23 Å). After the reaction, the C8−N9 has a double bond 1.30 Å and the C8−O8 a single bond (1.34 Å), since O8 has become protonated. Furthermore, when including the ZPE correction and also when applying the larger basis set (6-31+G(d,p)) the activation energy is decreased to 40.5 and 42.3 kcal/mol, respectively. Results from calculations of this reaction will be used as an unanalyzed reference, for more complex mechanisms that can be used to evaluate the catalytic effect.

Recalculating the reaction energy using the solvent model CPCM[29] gave almost an equal barrier.

Model C

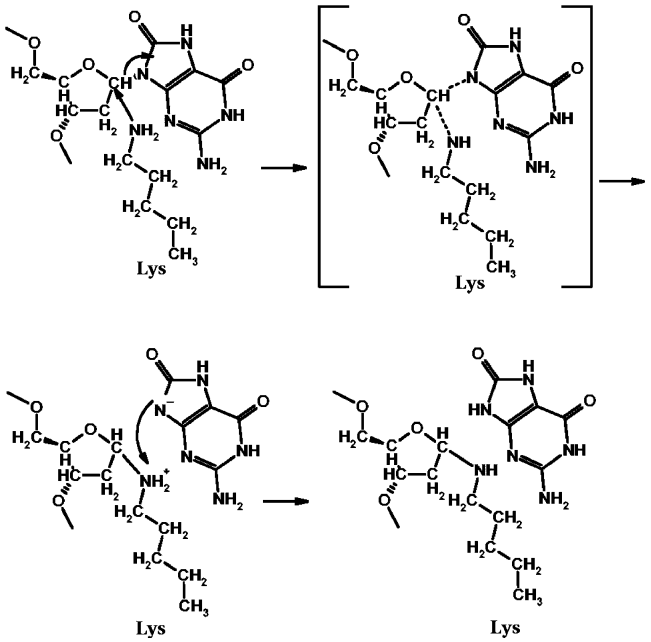

Figure 4. S_N2 reaction pathway C with lysine as an attacking nucleophile. The reaction scheme includes the TS structure.

S_N1 Pathway A. The position of Lys 249 was directly introduced in our model from the 1N3C structure. The NH_3^+ of the Lys 249 is positioned 3.98 Å from the C1′ and 3.18 Å from the N9. This reaction mechanism is more complicated than the other ones, with three separate reaction steps (see Figure 3). This mechanism has the highest reactant energy of the suggested reaction mechanisms presented here. The reactant energy of model A is 18.5 kcal/mol higher than model B's reactant energy. The binding of the reactants in the active site (not included) may lower this energy. But this is only an assumption we cannot confirm at this point. The NH_3^+ group of the Lys 249 stabilizes the dissociation of 8-oxoG since 8-oxoG becomes negatively charged during this reaction, with a first TS1 of 21.22 kcal/mol, relative the energy of the reactant. The first transition state (TS1) is reached when the C1′−N9 distance is 2.96 Å, and the NH_3^+ group is located near by the N9 of the 8-oxoG, see Figure 6. This leads to an intermediate at 19.00 kcal/mol above the reactant, where the N9 has formed a hydrogen bond with one of the hydrogen of the NH_3^+ group, with a negative 8-oxoG and a positive Deoxyribose. The NH_3^+ group of Lys 249 thereafter transfers one hydrogen to the N9 of the 8-oxoG with a second TS2 with a very low barrier to 19.20 kcal/mol and forms a second intermediate with an energy of 10.12 kcal/mol. If the deprotonated Lys 249 changes its conformation so that it is positioned on the opposite side under the C1′, no transition state could be found but a final product was formed spontaneously. The NH_2 of the Lys 249 binds to the C1′, and the final energy of the complex is −17.18 kcal/mol. The activation energy with ZPE correction is 18.6 kcal/mol, and for the larger basis set the activation energy is 20.2 kcal/mol. In both cases the energy deviation from the calculated barrier with the 6-31G(d) basis set are quite small, which probably means that the obtained results are stable. The major changes accurse for intermediate 1 and TS 2 with the corrected ZPE 16.3 and 14.4 kcal/mol respectively. Even when applying the larger basis set the energy shift remains but the difference is much smaller. It is possible that there is no second transition state for model A, but this problem has not been treated more carefully here since it does not affect our conclusions at this point.

S_N1 Pathway B. In the last case of the S_N1 reactions, the Lys 249 was introduced in the 1EBM structure, and the NH_3^+ group positioned within reach of the C1′ at a distance of 3.50 Å, but too far from the Asp 268 to become deprotonated. The NH_3^+ group of the Lys 249 is more or less a passive spectator while the 8-oxoG dissociates from the C1′ site; meanwhile, the C2′ of the Deoxyribose transfers one hydrogen to the O8 of the 8-oxoG. The TS energy in this reaction was found to be 48.94 kcal/mol, and a new intermediate is formed with the energy 27.31 kcal/mol. For the TS the C1′−N9 distance is 1.89 Å, which is an early TS compared with the other models presented here, also one hydrogen from the C2′ site is transferred to the O8. The ZPE corrected activation energy for this model was found to be 45.7 kcal/mol and with the larger basis set the energy was 46.0 kcal/ mol. This reaction is similar to the S_N1 Basic reaction, but with a higher energy barrier, which means that the Lys 249 has no or even an anti catalytic effect in this model. An explanation for this is that the positive NH_3 group of the Lys 249 is positioned far from the negative 8-oxoG with the cationic Deoxyribose as a shield between. During the reaction, only small changes in the position of the Lys 249 have been observed.

S_N2 Reaction. The alternative S_N2 reactions were investigated with two models of the Lys 249, both using the 1FN7 structure to position the attacking nucleophile, assuming that the Asp 268 or some other residue has deprotonated the NH_3 group of the Lys 249. In the first model, we used a reduced model of the lysine where it is only represented by an ammonia molecule, which has been shown to be able to cleave the 8-oxoG base.[30] In the other model, we keep the entire lysine chain.

S_N2 with NH_3. The Lys 249 has been replaced by an NH_3 group as an attacking nucleophile. The initial geometry from where the attack is taking place has been optimized. The NH_3 is positioned 3.21 Å from the C1′ and the NH_3 position seems to be stabilized by the O3′ of the sugar ring. When the NH_3 is attacking the C1′ site, the bond between C1′ and N9 breaks with a TS of 48.06 kcal/mol. At the TS, the distance for C1′−NH_3 is 2.12 Å and for C1′−N9 is 2.75 Å. Then an intermediate state at 41.36 kcal/mol above the reactant is formed when the NH_3 binds to the C1′, resulting in a negatively charged 8-oxoG and a positively charged NH_3 at C1′. Furthermore, the negatively charged 8-oxoG is then protonated at the N9 site by one of the hydrogen of the NH_3 and forms a stable product with energy of −5.34 kcal/ mol.

S_N2 Pathway C. In pathway C, the Lys 249 side chain, in the reactant geometry, is positioned with the NH_2 group 3.34 Å from the C1′; in the same way as ammonia, the NH_2 position of the Lys 249 is stabilized by the O3′ of the sugar ring. The reaction pathway is presented in Figure 4. When the NH_2 attacks the C1′ site, the 8-oxoG is replaced with a transition state energy TS of 46.46 kcal/mol, with the distances 2.20 Å (C1′−NH_2) and 2.66 Å (C1′−N9). The reaction proceeds to an intermediate state where the Lys 249 binds to the C1′ of the deoxyribose. The NH_2 of the Lys 249 is now positively charged, while the N9 of the 8-oxoG is negatively charged. The relative energy of the intermediate is calculated to be 36.50 kcal/mol. The reaction then goes spontaneously from the intermediate to the final product, transferring one hydrogen from the NH_2 to the N9 of 8-oxoG without any energy barrier if the 8-oxoG comes within 3.94 Å from the NH_2 group. The energy of the final product is −6.00 kcal/mol, which indicates that it is a stable form. To be able to transfer the hydrogen spontaneously,and form a product without any transition state, the Lys 249 or the scissile 8-oxoG needs to diffuse in the active site. This process could only be studied with a better model of the active site with the

TABLE 1: Calculated Reaction Energies (in kcal/mol)[a]

basis set	initial	TS 1	intermediat 1	TS 2	intermediat 2	product
			Basic			
6-31G(d)	0.0	45.3	–	–	–	25.4
ZPE 6-31G(d)	0.0	40.5	–	–	–	23.3
6-31+G(d,p)	0.0	42.3	–	–	–	20.8
			Model A			
6-31G(d)	0.0 (18.5)	21.2 (39.7)	19.0 (37.5)	19.2 (37.7)	10.1 (28.6)	−17.2 (1.3)
ZPE 6-31G(d)	0.0 (17.6)	18.6 (36.2)	16.3 (33.9)	14.4 (32.0)	6.9 (24.5)	−17.6 (0.0)
6-31+G(d,p)	0.0	20.2	17.9	17.8	8.5	−17.1
			Model B			
6-31G(d)	0.0	48.9	27.3	–	–	–
ZPE 6-31G(d)	0.0	45.7	25.0	–	–	–
6-31+G(d,p)	0.0	46.0	21.7	–	–	–
			Model C			
6-31G(d)	0.0	46.5	36.5	–	–	−6.0
ZPE 6-31G(d)	0.0	44.4	36.8	–	–	−5.7
6-31+G(d,p)	0.0	44.5	33.5	–	–	−5.8

[a] The values in parentheses are energies compared with Model B's initial state. The table also includes calculated zero-point corrected energies (ZPE).

TABLE 2: Transition-State Energy for the Extended System Calculated with Two Different Basis Set[a]

reaction step	basis set	Basic	model A	model B	model C
initial	6-31G(d)	0.0	0.0 (22.7)	0.0	0.0
	6-31+G(d,p)	0.0	0.0 (21.0)	0.0	0.0
TS	6-31G(d)	43.9	21.2 (43.1)	51.8	38.6
	6-31+G(d,p)	40.4	18.5 (39.5)	48.7	36.3

[a] All energies are in kcal/mol. The values in the parentheses are energies relative to model B's initial state. The models in this table refer to the extended system with the guanine instead of imidazole.

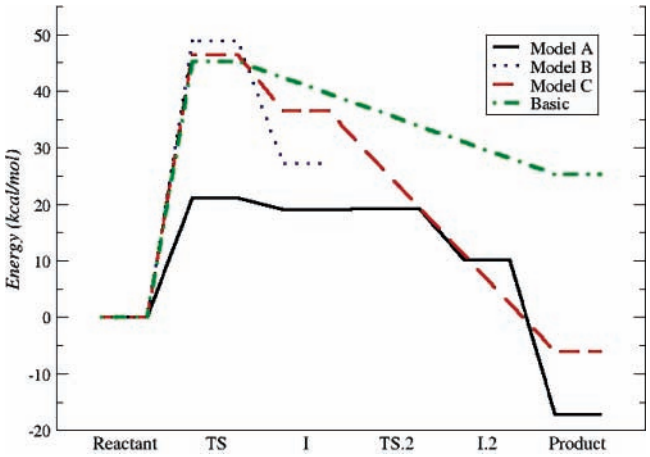

Figure 5. Energy comparison of the three different reaction pathways (A, B, and C), compared with the dissociation energy of 8-oxoG when the lysine is absent, referred in the graph as Basic. The reaction coordinate on the axis does not correspond to a specific structure and are different for each reaction pathway.

surrounding residues. The energy diagrams for the reaction and the transition state structure can be found in Figures 5 and 6. The effect of ZPE corrections and the use of the larger basis set 6-31+G(d,p) are fairly small (see Table 1). The only exceptions is the intermediate structure, which deviates about 3 kcal/mol when calculating it with the larger basis set, but still no major change. The change is probably due to the fact that the geometry was optimized with the smaller basis set (6-31G-(d)).

Extended Systems. In the previous sections, we have used a simplified model of 8-oxoG (oxidized imidazole); we are now recalculating the first TS energy for each reaction with the previously omitted part. For model C we made a new TS calculation after performing a geometry optimization of the new extended part, while the rest of the coordinate are fixed. We compared the new energy with the energy if we used the previous optimized TS structure for the simplified 8-oxoG. The energy difference was only 0.23 kcal/mol lower if we locked all other coordinates. So for the other reactions, we have taken the structures from previous calculations and optimized the geometry of the extended part. The result from these calculations is presented in Table 2. The TS energy for model A was almost unchanged (−0.84 kcal/mol), but more surprisingly, the change from imidazole to guanine lowers the energy barrier by 7.90 kcal/mol to 38.60 kcal/mol for model C. Furthermore, the energy barrier for the Basic model decreases to 43.93 kcal/ mol, while model B's energy barrier increases to 51.80 kcal/mol, which still indicates no catalytic effect. The increased energy difference between model C and Basic makes the S_N2 suggestion more probable, but still the energy barrier is more than 18.2 kcal/mol higher than that for the S_N1 reaction of model A. Recalculating the reaction energies with the basis set 6-31+G-(d,p) did not change the energy difference between the models but generally lowered the relative energies within the models. A detailed study of the energies can be viewed in the Table 2.

Properties. Properties such as proton affinity (PA) and charge distribution from the reactions have been analyzed and are presented in this section. The final product of 8-oxoG is not the same for all reaction pathways. There are two types of final products in our calculations. For the S_N1 reference and the B pathway, a hydrogen is transferred from C2′ to the O8 of the 8-oxoG; for the other reactions, both S_N1 (A) and S_N2 (C), one hydrogen is transferred to the N9 of the 8-oxoG (see Figures 3 and 4). We have compared the two different 8-oxoG products with the negatively charged 8-oxoG by performing an energy optimization. The 8-oxoG in our models is the oxo-imidazole. The PA of the negatively charged 8-oxoG with respect to O8 as protonation site has been calculated to 343.37 kcal/mol. If the protonation occurs at N9, the PA is 353.51 kcal/mol. Furthermore, the PA of the unmodified, negatively charged

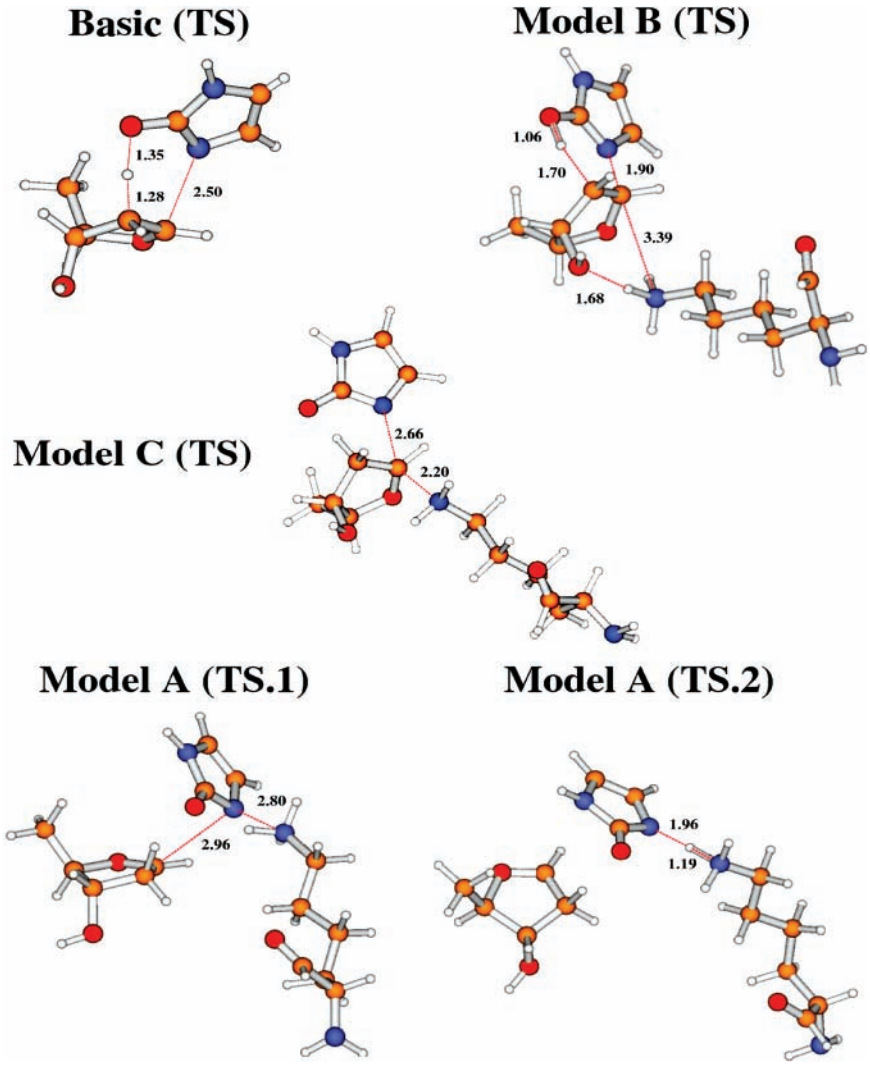

Figure 6. Transition state structures for each reaction, including a second TS (TS2) for model A.

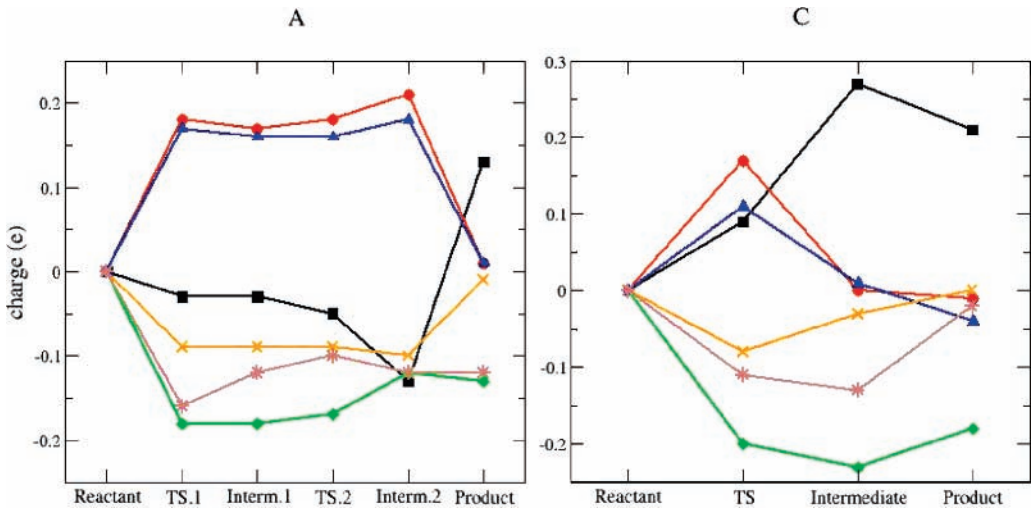

Figure 7. Charge distribution for reaction pathways A and C. The curves show the charge distribution for some atoms and it is the same selected atoms in both cases. The selected atoms are the nitrogen atom of the lysine's head (square), C1′ (circle), N9 (diamond), O4′ (triangle), C2′ (X), and O8 (star).

guanine (here imidazole) when N9 is protonated is obtained to 349.52 kcal/mol. Hence, the highest proton affinity was obtained for the product where the N9 of the negatively charged 8-oxoG is protonated. This would mean that the products from the pathway A and the different S_N2 pathways are energetically more favourable.

The atomic charge distributions during the reaction for pathways A and C are presented in Figure 7. The diagrams show how the charges change for each reaction step relative the initial step which is set to zero. The chosen atoms in the diagram are directly involved in the reactions or expected to be involved. The most interesting part of the diagrams, and what will be the

focus here, is the first transition state. The charge polarization gives us indications which transition state that could be most stabilized by the active site. At the first transition state, the charge distributions for both reaction pathways are quite similar except for the behavior of the N of the lysine's head in the S_N2. The reason for this is that the N of the lysine is attacking the C1′ of the sugar ring. Furthermore, the polarization of the O4′ and O8 is increased in pathway A compared with pathway C. This might indicate that the active site would stabilize pathway A's transition state structure more.

Summary of Results. The resulting energy barriers after calculating these small subsystems shows that the model A with the S_N1 reaction seems to be the most likely reaction, with an energy barrier of 21.2 kcal/mol, which is less than half of the dissociation energy needed with the reference model. Furthermore, in model B the lysine is revealed to have a small anticatalytic effect with a barrier that is 3.6 kcal/mol higher than the reference, while model C has almost the same barrier as the reference, and hence no large catalytic effect. For the extended system, where we used the whole 8-oxoG instead of oxidized imidazole as our 8-oxoG model, no dramatically changes were observed for model A and B compared with the extended reference model. But for the extended model C, the energy barrier decreased 5.3 kcal/mol relative to the extended reference model, which indicates that the lysine could be catalytic also in this reaction mode. Still the barrier for model A is 18.2 kcal/mol lower than model C. Another argument that support model A is the increased polarization of the O4′ and C1′ site at the transition state, compared with model C. This enables the prepolarized active site to interact stronger with the S_N1 transition state than with the S_N2, thus giving a stronger catalytic effect.

Conclusions

This study is an attempt to theoretically understand how the lysine participates in the reaction mechanism in which the hOGG1 enzyme excises the oxidated damaged guanine. Since this is the first study of this kind, to the best of our knowledge, it is essential to be able to follow and understand each step. The only way to do so, is to start with a system that is as small as possible without losing too much of the chemistry that we are looking for. The results presented in this article, and summarized in the previous section, give new strength to the argumentation for an S_N1 type of mechanism (model A in our article), but the possible importance of the surrounding residues in these types of reactions should be emphasized. The lysine electrostatically stabilizes the dissociating 8-oxoG and then donates one proton to the scissile 8-oxoG, and finally the lysine will form a Schiff base with the Deoxyribose. In the described reaction, the activation energy is 21.2 kcal/mol; this is less than half of the activation energy in the absence of lysine and hence reveals the catalytic effect of the lysine.

Preliminary results, from both molecular dynamic simulations[16,31] and recent crystallographic studies,[17] point toward an S_N1 mechanism. The S_N1 mechanism has been shown earlier to be relevant in enzymes with similar functions.[19] But still there are questions that cannot be answered with these models such as, Is it energetically favorable in the active site for the lysine to be positioned as in model A since the reactant energy is roughly 20 kcal/mol higher than that for the reactant in model B? In a forthcoming work, we hope to be able to resolve these questions after including the surrounding residues. Yet an alternative reaction mechanism has very recently been proposed by Stivers and Jiang, which includes a C1′−O4′ bond cleavage of the sugar ring before the 8-oxoG dissociate.[32] We also aim to compare this reaction with the results presented here.

Acknowledgment. This work has been supported by the Swedish Research Council, VR. A generous computing time allocation from HPC2N is gratefully acknowledged.

References and Notes

(1) Nash, H. M.; Bruner, S. D.; Scharer, O. D.; Kawate, T.; Addona, T. A.; Spooner, E.; Lane, W. S.; Verdine, G. L. *Curr. Biol.* **1996**, *6*, 968−980.
(2) der Kemp, P. A. V.; Thomas, D.; Barbey, R.; de Oliviera, R.; Boiteux, S. *Proc. Natl. Acad. Sci. U.S.A.* **1996**, *93*, 5197−5202.
(3) Lu, R.; Nash, H.; Verdine, G. *Curr. Biol.* **1997**, *7*, 397−407.
(4) Boiteux, S.; Radicella, J. *Arch. Biochem. Biophys.* **2000**, *377*, 1−8.
(5) Michaels, M.; Miller, J. *J. Bacteriol.* **1992**, *174*, 6321−6325.
(6) Thomas, D.; Scot, A.; Barbey, R.; Padula, M.; Boiteux, S. *Mol. Gen. Genet.* **1997**, *254*, 171−178.
(7) Bruner, S.; Norman, D.; Verdine, G. *Nature* **2000**, *403*, 859−866.
(8) Elahi, A.; Zheng, Z.; Park, J.; Eyring, K.; McCaffrey, T.; Lazarus, P. *Carcinogenesis* **2002**, *23*, 1229−1234.
(9) Friedberg, E.; Walker, G.; Siede, W. *DNA Repair and Mutagenesis*; ASM Press: Washington, DC, 1995.
(10) Grollman, A.; Moriya, M. *Trends Genet.* **1993**, *9*, 246−249.
(11) Hainaut, P.; Hernandez, T.; Robinson, A.; Rodriguez-Tome, P.; Flores, T.; Hollstein, M.; Harris, C.; Montesano, R. *Nucleic Acids Res.* **1993**, *26*, 205−213.
(12) Hollstein, M.; Greenblatt, M.; Soussi, T.; Hovig, E.; Montesano, R.; Harris, C. C. *Nucleic Acids Res.* **1996**, *24*, 141−146.
(13) Bjørås, M.; Seeberg, E.; Luna, L.; Pearl, L.; Barrett, T. *J. Mol. Biol.* **2002**, *317*, 171−177.
(14) von Hippel, P. H.; Berg, O. H. *J. Biol. Chem.* **1989**, *264*, 675−678.
(15) Panayotou, G.; Brown, T.; Pearl, L. H.; Savva, R. *J. Biol. Chem.* **1998**, *273*, 45−50.
(16) Pinak M. *J. Mol. Struct. (THEOCHEM)* **2002**, *583*, 189−197.
(17) Norman, D. P. G.; Chung, S. J.; Verdine, G. L. *Biochemistry* **2003**, *42*, 1564.
(18) Fromme, J. C.; Bruner, S. D.; Yang, W.; Karplus, M.; Verdine, G. L. *Nat. Struct. Biol.* **2003**, *10*, 204.
(19) Dinner, A.; Blackburn, G.; Karplus, M. *Nature* **2001**, *413*, 752.
(20) Nash, H. M.; Lu, R.; Lane, W. S.; Verdine, G. L. *Curr. Biol.* **1997**, *4*, 6693−702.
(21) Norman, D. P. G.; Bruner, S. D.; Verdine, G. L. *J. Am. Chem. Soc.* **2001**, *123*, 359.
(22) Frisch, M. J.; Trucks, G. W.; Schlegel, H. B.; Scuseria, G. E.; Robb, M. A.; Cheeseman, J. R.; Zakrzewski, V. G.; Montgomery, J. A., Jr.; Stratmann, R. E.; Burant, J. C.; Dapprich, S.; Millam, J. M.; Daniels, A. D.; Kudin, K. N.; Strain, M. C.; Farkas, O.; Tomasi, J.; Barone, V.; Cossi, M.; Cammi, R.; Mennucci, B.; Pomelli, C.; Adamo, C.; Cli.ord, S.; Ochterski, J.; Petersson, G. A.; Ayala, P. Y.; Cui, Q.; Morokuma, K.; Malick, D. K.; Rabuck, A. D.; Raghavachari, K.; Foresman, J. B.; Cioslowski, J.; Ortiz, J. V.; Baboul, A. G.; Stefanov, B. B.; Liu, G.; Liashenko, A.; Piskorz, P.; Komaromi, I.; Gomperts, R.; Martin, R. L.; Fox, D. J.; Keith, T.; Al-Laham, M. A.; Peng, C. Y.; Nanayakkara, A.; Challacombe, M.; Gill, P. M. W.; Johnson, B.; Chen, W.; Wong, M. W.; Andres, J. L.; Gonzalez, C.; Head-Gordon, M.; Replogle, E. S.; Pople, J. A. *Gaussian 98*, revision a.9; Gaussian, Inc.: Pittsburgh, PA, 1998.
(23) Becke, A. *Phys. Rev. A* **1988**, *38*, 3098.
(24) Becke, A. *J. Chem. Phys.* **1993**, *98*, 1372−1377.
(25) Lee, C.; Yang, W.; Parr, R. *Phys. Rev. B* **1988**, *37* (2), 785−789.
(26) Ayala, P. Y.; Schlegel, H. B. *J. Chem. Phys.* **1997**, *107*, 379−384.
(27) Reed, A. E.; Curtiss, L. A.; Weinhold, F. *Chem. Rev.* **1988**, *88*, 899−926.
(28) Blomberg, M. R. A.; Siegbahn, P. E. M. *J. Phys. Chem.* **2001**, *105*, 9375−9386.
(29) Barone, V.; Cossi, M. *J. Phys. Chem.* **1998**, *102*, 1995−2001.
(30) Meyer, C.; Meyer, D.; Bickle, T.; Giese, B. *ChemBioChem* **2003**, *4*, 610−614.
(31) Pinak, M. *Comput. Biol. Chem.* **2003**, *27*, 431−441.
(32) Stivers, J. T.; Jiang, Y. L. *Chem. Rev.* **2003**, *103*, 2729−2759.